buildings

MDPI

Article

Verification of the Maximum Stresses in Enhanced Welded Details via High-Frequency Mechanical Impact in Road Bridges

Hassan Al-Karawi [1,*], John Leander [2] and Mohammad Al-Emrani [1]

[1] Architecture and Civil Engineering Department, Chalmers University of Technology, 412 96 Gothenburg, Sweden
[2] Structural Engineering and Bridges, Royal Institute of Technology (KTH), 114 28 Stockholm, Sweden
* Correspondence: hassan.alkarawi@chalmers.se; Tel.: +46768504139

Abstract: High-frequency mechanical impact (HFMI) is an efficient post-weld treatment technique that enhances fatigue strength in metallic welded structures. Steel or steel-concrete composite road bridges, where the fatigue limit state often governs the design, compose one category of structures that can benefit from the application of this technology. To assert an improvement in fatigue strength using HFMI, the induced compressive residual stresses must be stable. Therefore, the maximum service stresses that can be allowed on HFMI-treated joints should be controlled to avoid the relaxation of the induced beneficial compressive stresses by HFMI treatment. Using statistical analysis of recorded traffic, this paper compares the measured maximum traffic loads to those generated by a load model. More than 870,000 and 470,000 recorded vehicles from traffic measurements in Sweden and the Netherlands are used in this analysis. To capture the characteristic bending moment, the daily maxima of the resulting measured load effect are combined with the extreme value distribution of the bending moment. In addition, it is found that the characteristic load combination is the best-studied option to assess the maximum stress in HFMI-treated weldments in road bridges.

Keywords: road bridges; weight in motion; HFMI treatment; design; peak over threshold; Gumbel distribution; Eurocode

Citation: Al-Karawi, H.; Leander, J.; Al-Emrani, M. Verification of the Maximum Stresses in Enhanced Welded Details via High-Frequency Mechanical Impact in Road Bridges. *Buildings* **2023**, *13*, 364. https://doi.org/10.3390/buildings13020364

Academic Editor: Harry Far

Received: 11 January 2023
Revised: 20 January 2023
Accepted: 25 January 2023
Published: 28 January 2023

1. Introduction

High-frequency mechanical impact (HFMI) treatment is a relatively recent method that can significantly increase steel weldments' fatigue strength. In contrast to other post-weld treatment techniques, HFMI treatment is an eco-friendly, simple, quick, efficient, and reasonably priced technique [1,2]. The treatment creates a better weld-toe transition, which leads to local material hardening and topographic changes [3]. However, the treatment mainly affects the welded region by removing the tensile welding residual stress and replacing it with a more beneficial compressive residual stress [4]. In order to assert an improvement in fatigue strength, the stability of these beneficial compressive stresses should be ensured through the design life of the structure [5].

Several rigorous fatigue testing studies investigated the stability of HFMI-induced compressive residual stresses [6–8]. The application of high mean stress, high-stress range, or high maximum stress is found to cause a significant reduction of fatigue strength of HFMI-treated welds because of compressive residual stress reduction, or even elimination in some cases [8]. The is not the case in conventional welds (i.e., not HFMI-treated) as the load conditions are assumed to have no influence on the fatigue strength as high tensile residual stress is already assumed at the weld toe. Therefore, some design checks should be made to ensure that load effects, during the structure's service life, do not exceed certain allowable limits. These limits were found to be related to both the structural detail type (the severity of stress concentration for the particular detail) and the yield strength of steel according to the International Institute of Welding (IIW) assigns some of these limits for

various structural details covered by this guideline [9]. For instance, the limitations on the maximum constant amplitude stress range that can be applied to a weld so that the benefit from HFMI treatment can be claimed are assigned depending on the yield strength and the stress ratio of the loading cycle [9].

In addition to that, the effect of high mean stress on the fatigue strength of HFMI-treated details is usually considered by assigning lower fatigue strength depending on the stress ratio of the load cycles [9,10]. This is rather straightforward when the fatigue load is of constant amplitude with a defined stress ratio. For variable amplitude loading where both the stress range and the mean stress change, an equivalent load magnification factor (λ_{HFMI}) has been proposed to consider the variations in load characteristics including the effect of the bridge self-weight. Models for λ_{HFMI} have been proposed in a previous work based on calibration against real traffic loading [5,11]. This includes applications for steel and steel-concrete road bridges. Similar work is ongoing to propose similar expressions for railway bridges.

As mentioned before, the beneficial compressive residual stress induced by HFMI treatment exhibits sensitivity to possible overloads in variable amplitude [12–16]. Several experimental studies have shown that the limits of permissible overloads beyond which the effect of HFMI treatment begins to decline depending on the type of detail (reflecting the severity of stress concentration at crack initiation points) and the yield strength of the material [12,15,16]. This has, for example, been recognized by the German standards for steel structures, DASt-Richtlinie [10] where the maximum permissible stresses on three typical welded details are specified; see Equations (1)–(3). These details are butt-welded, transverse, and longitudinal welded attachments. With that, the question of how to incorporate these constraints into design becomes imminent. In other words, which loads, or load combinations should be used by the designer in order to check these limits? To the best of the author's knowledge, no light has been thrown on this issue before.

$$\text{Fy} > \text{Smax} > -0.5\ \text{Fy Longitudinal attachment} \quad (1)$$

$$\text{Fy} > \text{Smax} > -0.7\ \text{Fy Transversal attachment} \quad (2)$$

$$\text{Fy} > \text{Smax} > -0.9\ \text{Fy Butt welds attachment} \quad (3)$$

This study aims at providing a basis on which the verification of the maximum permissible load effect in HFMI-treated welded joints existing in road bridges can be made. This includes any welded details in road bridges, such as transverse attachments, longitudinal attachments, butt welds, and others. The focus is not on the allowable limits of the maximum stresses in HFMI-treated weldments because such limits are already provided for different detail types in Equations (1)–(3). Therefore, this paper focuses on how to conduct the verification of the maximum stresses in road bridges using these equations. Three load combinations according to the Eurocode are examined: The frequent or characteristic load combination associated with the serviceability limit state check, and the ultimate limit state combination. Characteristic bending moment values for a one-year reference period were estimated using measured vehicles by the weight-in-motion method.

The peak-over-threshold method (POT method) is used to produce extreme value distributions (Gumbel distribution) of the load effect over the selected reference period. Some information about the method can be found in [17]. Data from more than 470,000 heavy vehicles in the Netherlands and more than 872,000 vehicles in Sweden to generate these distributions are used in this study. In addition, two composite concrete-steel bridges in Sweden with various span lengths and support conditions are analyzed. For designers to perform the verification easily, the resulting load effect is compared to load model 1 which is often used to account for the traffic load effect in the Eurocode.

2. Methods

2.1. Traffic Measurements

The Swedish transport administration (Trafikverket) provided a data set with information on more than 872,000 vehicles. The traffic data were recorded over a period of 584 days using the weight-in-motion method. The data are based on repeated traffic measures collected between 2005 and 2009. Axle loads and the distance between every two adjacent axles are included in the data files to enable the calculation of the bending moment. The time of measurement is also important to allow data sortation in subsequent steps. Additional information about the measured data can be found in [18].

In addition to the Swedish data pool, more measurements of axle loads and configurations from the Netherlands were also obtained using the weigh-in-motion method. The measurement was performed on the A16 motorway in April month in both 2008 and 2018. The interested readers are referred to [19] where both data pools are described in more detail. The weight-length distribution of the different measured data pools is given in Figure 1. Besides, Table 1 also displays the size and vehicle types in each data pool.

In the first step of the analysis, bending moment influence lines were generated for different sections along several bridge beams with different influence line lengths from 10 to 80 m. The selected sections are the mid-span and over the support, and at a distance of 0.15 L and 0.25 L from the intermediate support in a two-spanned continuous bridge with identical span lengths. Additionally, one more section is considered at the midspan of a simply supported bridge where the bending moment is the highest.

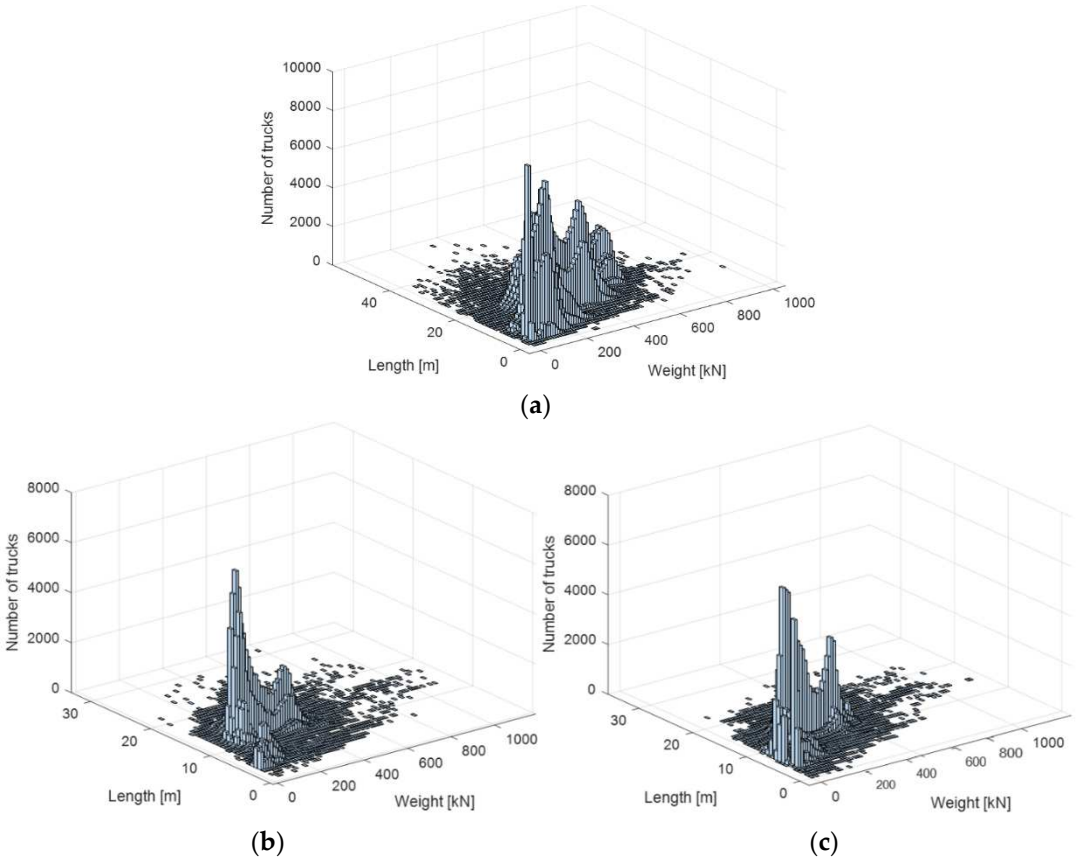

Figure 1. Weight-length distribution of the studied traffic pool (**a**): Swedish data measured in 2005-2009, (**b**): Dutch data measured in 2008, (**c**): Dutch data measured in 2018.

Table 1. Number of lorries in each data pool (×1000).

Number of Axles	Swedish Data [18]	Dutch Data 2008 [19]	Dutch Data 2018 [19]
Measuring days	584	30	30
2-axles vehicles	173	29	21
3-axles vehicles	109	15	14
4-axles vehicles	80	58	56
5-axles vehicles	189	120	112
6-axles vehicles	110	14	15
7-axles vehicles	179	1	2
8+axles vehicles	33	1	1
Total	873	238	221

In total, 40 bridge cases were analyzed comprising one section each for simply supported bridges and four sections in continuous bridges. These cases are chosen as reference points, whereas steel weldments can be present anywhere along the bridge axis based on design or construction purposes. The bending influence factor generated by the passage of a reference load of 1 unit is given in Figure 2. The influence factor is normalized to the maximum value (which corresponds to the midspan in the simply supported bridge).

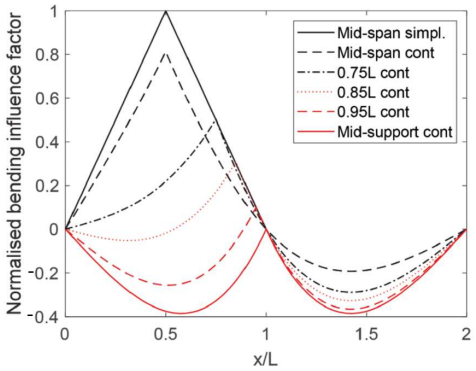

Figure 2. Bending influence factors the different positions. x & L give the position on the point load from the left edge and the span length respectively.

2.2. Statistical Distributions

For variable action (such as traffic loads), the load is defined by its characteristic value, which in Sweden is the 98th percentile of the annual maximum distribution equivalent to a 50-year return period for bridge design [20]. Towards the aim of this paper, one goal is to characterize the maximum bending moment experienced during the reference period. For this purpose, extreme value analyses need to be performed in terms of maximum bending moment in all studied bridges and sections using the measured traffic data in both countries. Gumbel distribution is one extreme value distribution that can describe the maximum sectional forces (shear force or bending moment) caused by vehicles' movement on highway bridges [20]. However, with the limited data currently available, it is not possible to identify the requisite amount of data to directly establish the Gumbel distribution parameters. As a result, statistical extrapolation should be applied [20].

One question that needs to be addressed is what type of data should be utilized to indicate extreme bending moments. One possible alternative is the division of the available data in each pool into blocks, each block represents one day of measurement. This explains why the date of measurement was retrieved. The maximum generated bending moment in each measurement day (daily maxima) is then evaluated, as shown in Figure 3. The following step involves selecting a threshold so that the mean excess shows linearity with the threshold value. A few illustrations of this linearity are shown in Figure 4. The data above the threshold are then fitted to an exponential distribution. The threshold is then

adjusted to enhance the fitting's quality. It is found that a threshold set to be the 30–50th percentile gives the best fit.

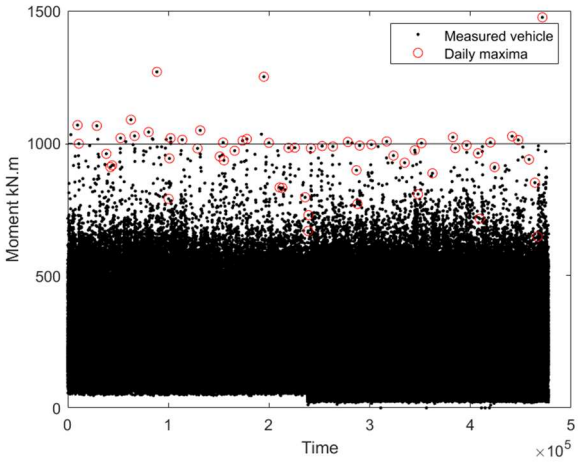

Figure 3. Example showing the extraction of the daily maxima, with an assumed threshold of 1000 kN.m. The *x*-axis gives the order of vehicles in the data pool.

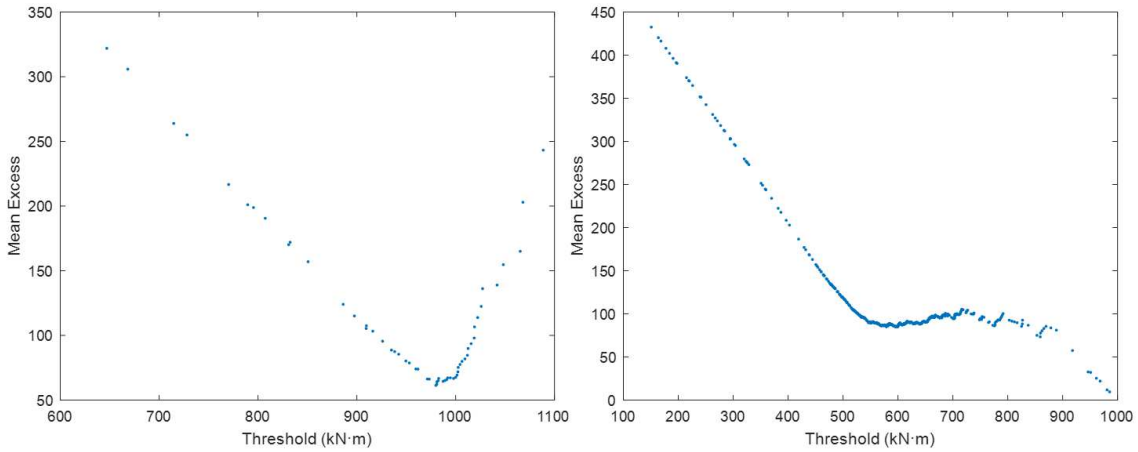

Figure 4. Examples of plots showing the mean exceedance versus the threshold level. The plots show a linear behavior below threshold values of 980 and 579 respectively.

The intensity of vehicles above the threshold is then determined for the selected reference period (one-year). The threshold value (u), the exponential distribution parameter (m), and the intensity of exceedance (λ) are used to determine the Gumbel distribution (see Equation (4)), which gives the cumulative distribution function (CDF) in terms of these three parameters. Finally, the characteristic value is calculated to be the 98th percentile of this function, as shown in Equation (5).

$$F(x) = \exp(-\exp((x\text{-}u\text{-}m \cdot \ln(\lambda)/m))) \quad (4)$$

$$M_{Char} = F^{-}(98\%) \quad (5)$$

2.3. Comparison to Load Model

Stresses acting on steel weldments in composite bridges include permanent load due to self-weight, traffic load, thermal load, and stresses due to concrete creep and shrinkage [21]. The calculation of these stresses yields results which are usually close to reality. The only possible exception is the traffic load where the load model might differ significantly from the real measured traffic. Therefore, the extreme value analysis can be limited to traffic load effects, where the characteristic value of the bending moment obtained from the

statistical analysis is compared to the bending moment obtained from load model 1 (LM1) in Eurocode [21].

Load model LM1 consists of both concentrated and distributed loads considered in different lanes, as shown in Figure 5. LM1 is chosen because engineers need to calculate it in a conventional design procedure for verifications at ultimate and serviceability limit states (characteristics, quasi-permanent & frequent combinations). LM1 can also be used for fatigue verification for infinite life assumption [21]. Therefore, the comparison is made with respect to these three combinations according to Equation (6). The multipliers given in the equation vary depending on the considered combination as given in Table 2.

$$M_{Char} < \gamma_Q \, \gamma_1 \, M_{LM1} \tag{6}$$

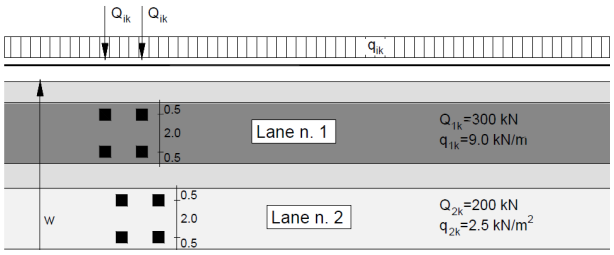

Figure 5. Eurocode LM1 in Eurocode 1991–1992 [21].

Table 2. Multipliers used for different combinations.

State	Ultimate Limit State	Serviceability Limit State	
		Frequent Combination	Characteristic
γ_Q	1.5	1	1
Ψ_0	1	0.75 or 0.4 *	1

*: $\Psi_0 = 0.75$ is applied for the point load, and $\Psi_0 = 0.4$ for the distributed load.

It is important to note that, depending on the number of lanes, LM1 can have a different load configuration than that seen in Figure 5. Herein, two lanes are considered. Besides, the distributed load is considered only where it gives an unfavorable effect. In other words, the distributed load is considered where it produces a negative moment over the support and at 0.15 L from the intermediate support, or a positive moment at the midspan and at 0.25 L from the intermediate support, see Figure 2. In addition, it should be kept in mind that this load model implicitly includes the dynamic amplification factors.

2.4. Case Study Bridges

Since the first step of the analysis, given in the previous section, considers only the moment due to traffic load, additional analysis is made here to consider the other stresses which include the permanent load, such as self-weight, thermal load, wind load, and stress rises due to concrete shrinkage. Two composite concrete-steel case study bridges built and designed in Sweden are investigated to examine the different load combinations (Frequent SLS, Characteristic SLS and ULS). The bridge spans together with the studied welded details are given in Figures 6 and 7. Table 3 gives the coordinates of the constructional details with respect to the bottom flange at the external support. The calculated combined stresses are then compared to the maximum permissible stress limits given in Equations (1)–(3) which should not be exceeded when HFMI treatment is to be used for fatigue strength enhancement. In this paper, the stresses are calculated at the extreme fibres of the whole bridge length, and where the structural welded details exist. It is worthy to mention that the constructional details shown in Figures 6 and 7 are not in the original design documents, but assumed here for illustration. The consideration of load effects is given in Appendix A.

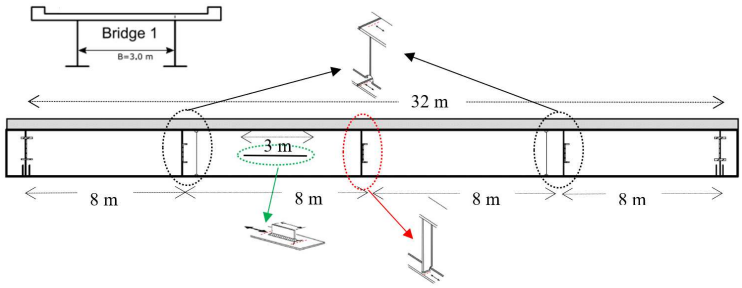

Figure 6. Case-study simply supported bridge (bridge 1).

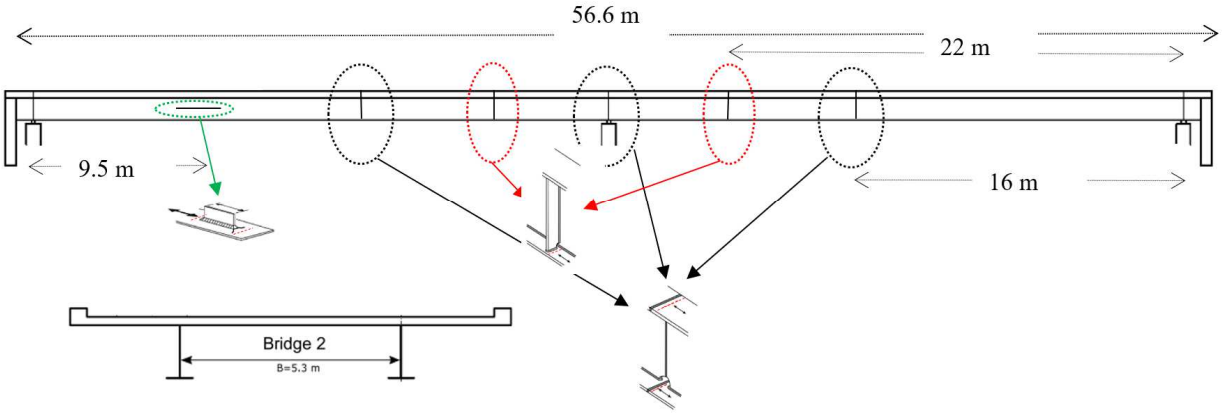

Figure 7. Case-study continuous bridge (bridge 2).

Table 3. Multipliers used for different combinations.

Detail Type	x-Coordinate (m)	y-Coordinate (mm)
Simply supported bridge (bridge 1)		
1.Butt-weld	8	0, 1360 *
2.Longitudinal attachment	10.5	750
3.Longitudinal attachment	13.5	750
4.Transverse attachment	16	20
5.Butt-weld	24	0, 1360 *
Continuous bridge (bridge 2)		
1.Longitudinal attachment	7	850
2.Longitudinal attachment	10	850
3.Butt-weld	16	0, 1250 *
4.Transverse attachment	22	40
5.Butt-weld	28.3	0, 1250 *
6.Transverse attachment	34.6	40
7.Butt-weld	40.6	0, 1250 *

* Two welded details here, one on the bottom flange, and one on the top flange.

Both case-study bridges are made of S355 structural steel. These bridges are made of double I-girders supporting a reinforced concrete slab made of C35/45 concrete. The first bridge is a simply supported highway bridge with a span length of 32 m, constructed over E4 in Skulnäs. The second bridge is a double-span bridge constructed in Viskan with a total length of 56.6 m. The cantilever distances of the cross-sections are 1 m and 1.5 m for bridges 1 and 2 respectively. More information about these bridges can be found in [22,23]. The methodology followed in this paper is summarized in the flowchart given in Figure 8.

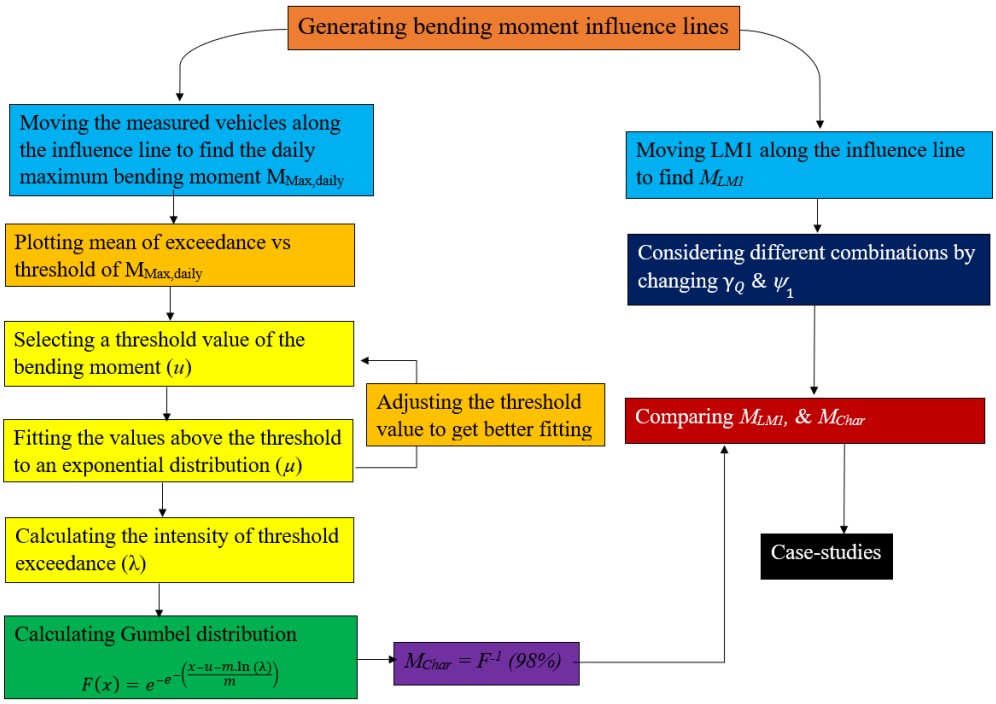

Figure 8. Summarized paper's methodology.

3. Results

A sample of the cumulative distribution functions (CDF) of the obtained Gumbel distribution is given by the solid curve shown in Figures 9 and 10. These figures also show the empirical CDF of the daily maxima (x-marked curve) and all the vehicles (dotted curve). The number of data points is 584 for the Swedish data and 60 for the Dutch data, respectively, reflecting the number of measurement days. The exponential distribution fitted to the data above the threshold (circles) is plotted on the same figure. The figure demonstrates that the fitting of the exponential distribution curve is quite successful. Only the daily maxima above the threshold are plotted in this instance. Additionally, as shown in Figure 3, most of the daily maxima are among the absolute maximum bending moments, making the usage of the daily maxima as an object for extrapolation choice in the POT approach justifiable.

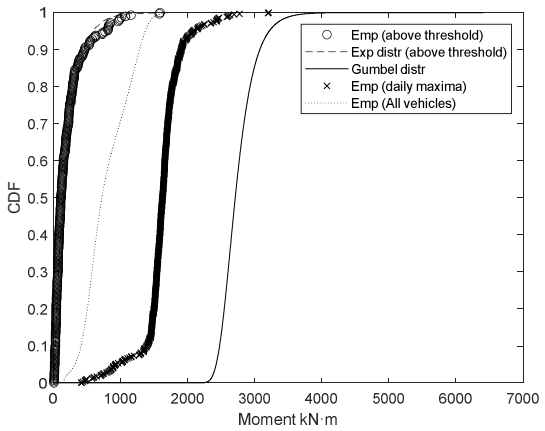

Figure 9. Example of the cumulative distribution function of Gumbel distribution (Swedish data, L = 20 m, Midspan section.

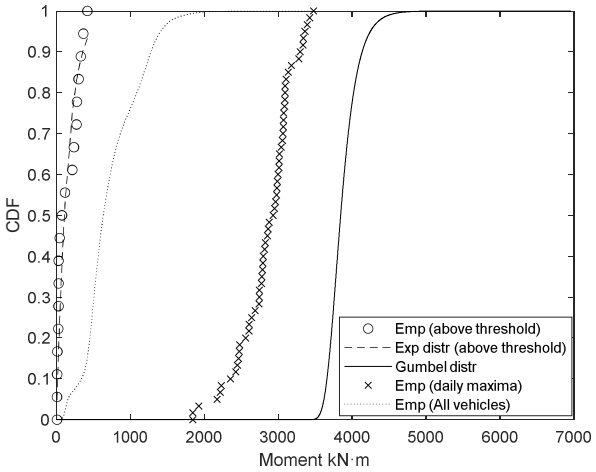

Figure 10. Example of the cumulative distribution function of Gumbel distribution (Dutch data, L = 20 m, Midspan section).

Figure 11 illustrates the characteristic value of the derived Gumbel distribution for both Swedish and Dutch traffic for various span lengths and positions. Besides, Figures 9–11 demonstrate that Dutch traffic generates larger bending moments than Swedish traffic, which may be related to the former heavier traffic. This is further demonstrated in Figure 1 which shows that the Dutch pool contains a significant number of vehicles heavier than 1000 KN which is not the case for the Swedish pool. This is because the Dutch data include some exceptional transport with heavy vehicles which requires a special permit.

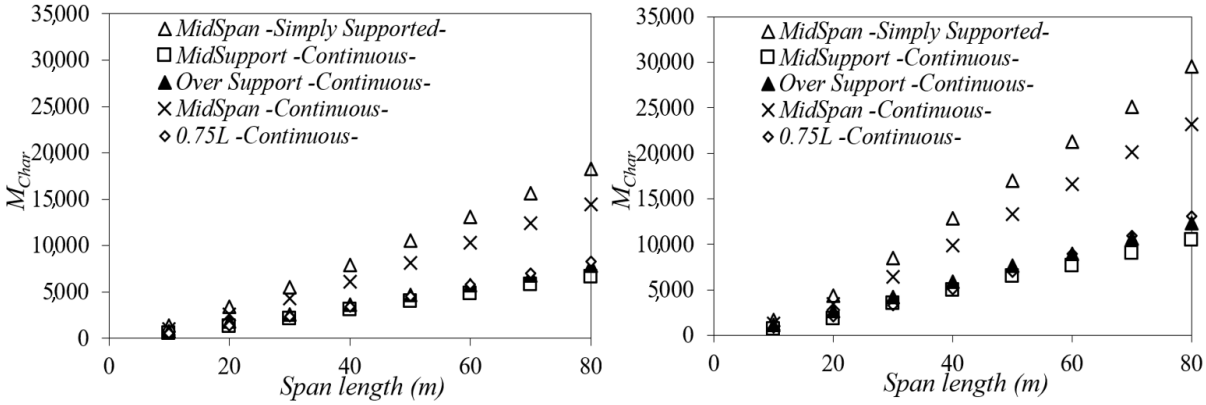

Figure 11. Characteristic traffic bending moment (98th percentile) of the Swedish and Dutch traffic respectively.

The characteristic moments in both countries can then be compared to the bending moment generated by LM1 considering the multipliers in Table 1 for frequent, characteristics, and ultimate limit combinations. The results are shown in Figure 12. Herein, M_{Char} of the Swedish traffic can be conservatively represented by the frequent combination, while the characteristic combination significantly overestimates it. On the other hand, the Dutch traffic is underestimated by up to 40% by LM1 in the frequent combination, while the characteristic combination appears to be more appropriate here with less than 10% underestimation in the 0.85 L continuous bridge case. For both traffic pools, the ULS load is too much on the safe side, which makes it not the best choice. Therefore, SLS (characteristic combination) is more appropriate to verify HFMI-treated details in road bridges.

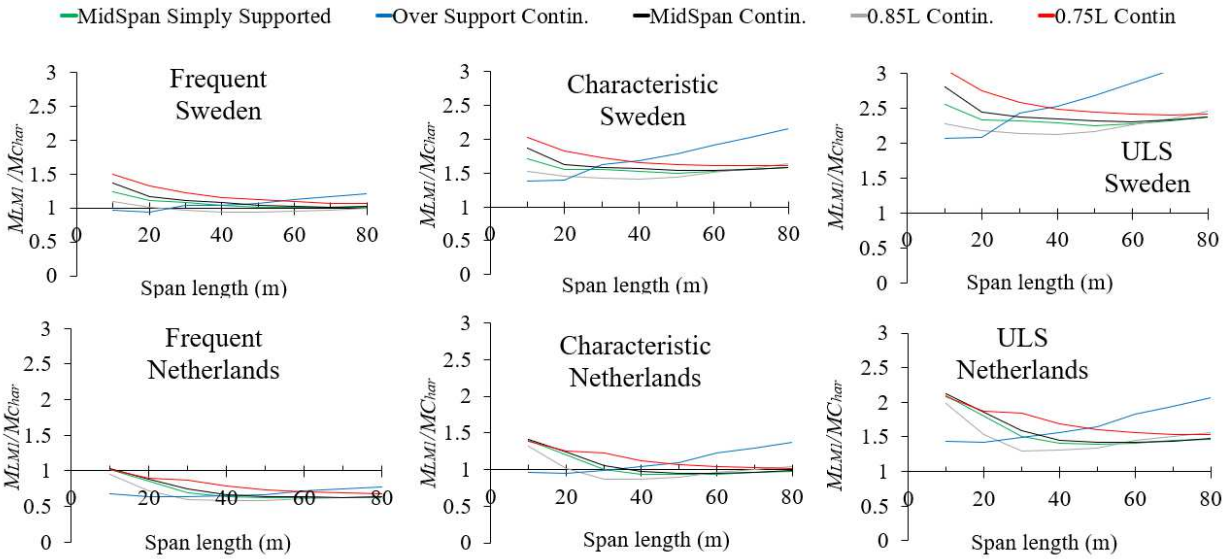

Figure 12. M_{LM1}/M_{Char} for the Swedish & Dutch measured traffic (**Top** & **Bottom**). **Left**: Frequent SLS, **Middle**: Characteristic SLS, **Right**: ULS.

Since both frequent SLS combinations and ULS either underestimate or overestimate the traffic load significantly as shown in Figure 12, they will be excluded from the stress analysis of the two case-study bridges given in Section 2.4. Therefore, only the characteristic SLS combination is considered, as shown in Figure 13. Equation (7) gives the loads included in this combination. It is noteworthy that other possible equations might need to be checked to include different traffic load models such as LM2 (which accounts for the single axle) or LM4 (which accounts for crowd loading) in the SLS check. However, Equation (7) gives the highest stresses, which the designers need to check always. The variables G, and S in the equation refer to the self-weight stress and stress raising due to the shrinkage of concrete. T_k and F_W refer to the thermal stress and stress due to wind load. Besides, TS and UDL are the stresses due to concentrated and distributed forces in LM1.

$$\text{Characteristic stress} = G+(0 \text{ or } 1)S + TS + ULD+0.6 \max (F_W, T_k) \quad (7)$$

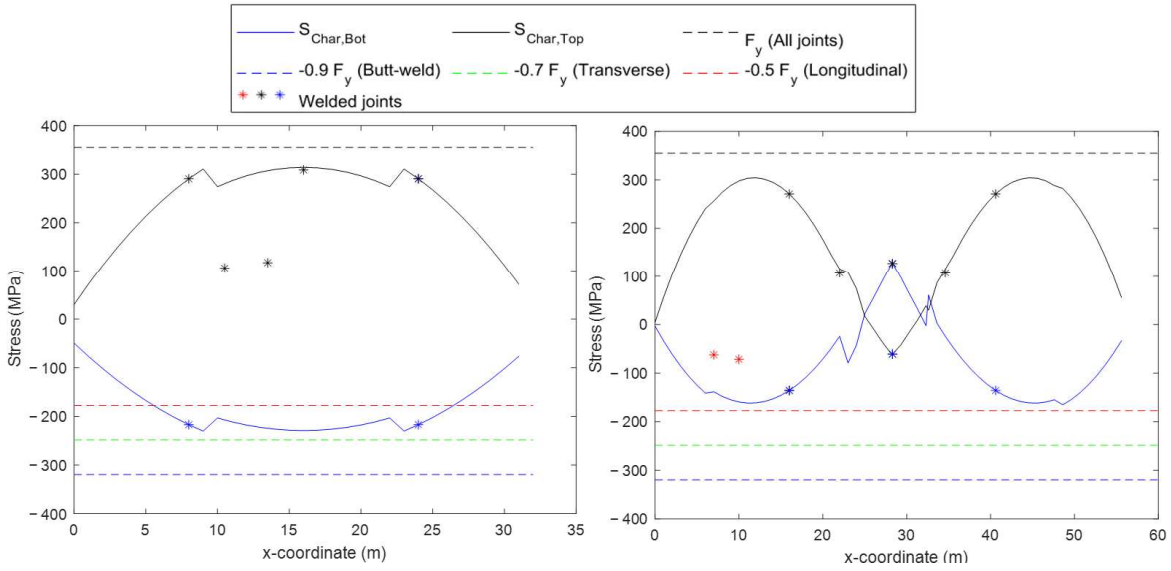

Figure 13. Characteristic SLS combination stresses of the two case study bridges.

Figure 13 shows that, for the combined loads, the tensile stress does not reach the assigned limit for all details (1.0 Fy = 355 MPa) in both studied cases. Besides, the compressive stresses do not reach the limits given for the butt-weld joints and the transverse attachment (−0.9 Fy and −0.7 Fy). On the other hand, the calculated compressive stresses do exceed the limit assigned for the longitudinal attachments in the simply supported bridge by up to 27% in some locations along the bridge. Nonetheless, it should be remembered that these stresses are calculated at the extreme fibers where longitudinal attachments are not placed usually.

In fact, the bending stresses due to major actions, such as permanent and traffic loads, will be smaller at the position of these attachments as these types of details are usually located in the web and terminate close to the neutral axis. This is clear in the figures which show that both the tensile and compressive stresses on the existing longitudinal attachment do not exceed ±0.3 Fy. In addition, LM1 overestimates the bending moment more than real traffic if a characteristic SLS combination is considered, as shown in Figure 12. Therefore, the maximum stress effect is not limiting the use of HFMI treatment in these bridges.

4. Discussion

In this paper, a verification format for the maximum stresses in HFMI-treated weldments in concrete-steel composite bridges is suggested. This is performed by comparing the real traffic data measured in two different countries and extrapolated using statistical analyses, to the traffic load model suggested in the Eurocode for vehicles. Different factors and multipliers are considered, and those corresponding to the characteristic combination in the serviceability limit state were found to be the most adequate for verification.

One important question is why the study focuses on the traffic loads more than the rest of the loads that are considered in the load combination, such as environmental loads (wind, temperature variation) and permanent loads. In fact, the model uncertainty for permanent loads is smaller than those corresponding to environmental or traffic loads [24]. This motivates the higher partial factors corresponding to the variable loads (γ_Q = 1.5). Besides, despite that the model uncertainty suggested for reliability-based analyses are in the same range for traffic as for environmental load [24], traffic often has a more prominent influence, which makes the uncertainty related to traffic the most influential.

Since the Gumbel distribution is derived from the daily maxima, which belong to the absolute maximum values of bending moment as shown in Figure 3, the sensitivity to the selected threshold is not very significant. Figure 14 shows an example of such a sensitivity for traffic load from both countries. For Swedish traffic, the results are even less sensitive, and no significant difference is found for selected threshold values set to be up to 80% of the daily maxima. For Dutch traffic, since the pool size is smaller, and the number of measurement days is less, the results become more sensitive to the threshold value, and the threshold should be selected more carefully.

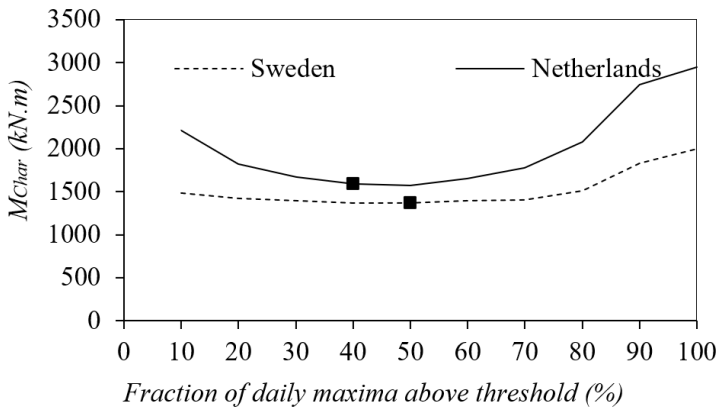

Figure 14. Sensitivity of the characteristic bending moment to the threshold value (L = 10 m, MidSpan section).

Structural safety considerations must be associated with a reference period. It all comes down to the accepted probability of failure over a given period. Figure 15 shows an example of the reference period effect on the characteristic value. As the reference period becomes longer, the probability of heavier vehicle passage increases which causes M_{Char} to increase. One year is the natural choice since environmental actions can be assumed independent between different years. The characteristic values can be defined for a selected probability (or an associated return period), which, in Sweden, is set to the 98th percentile for variable loads.

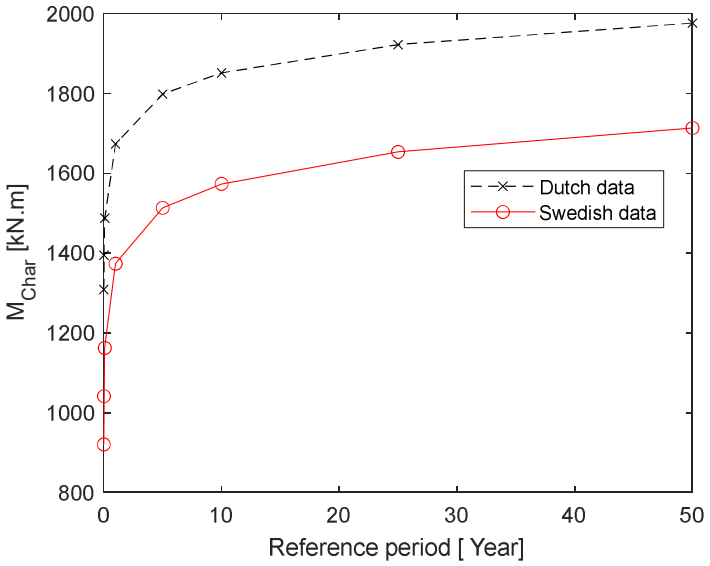

Figure 15. Example of the reference period effect on M_{Char} (L = 10 m, MidSpan section).

Since the results obtained in this paper are based on vehicle measurements, they cannot be generalized to railway bridges. A similar analysis could be conducted for the bending moment generated by the passage of measured trains on some case-study bridges. Then, the moment values can be compared to the load model LM71 considering the multipliers for characteristic combinations. Railway bridges are less likely to experience the same type of overloads as for road bridges. Nonetheless, more research is encouraged to verify that the characteristic combination of actions can be used for verification.

HFMI treatment is a technique that can be used in different industries where welding is involved. Therefore, the verification formats of the maximum stresses to attain the beneficial compressive residual stresses can be studied in the same way as for weldments in road bridges. This includes other bridge types (railway or pedestrian bridges), cranes, automobiles, and offshore structures. However, this requires realistic in-service stress assessment using real measured loads which are relevant for these structures.

5. Conclusions

HFMI treatment is a promising post-weld treatment method that can be used to enhance the fatigue strength of steel weldments in steel and composite bridges. One issue that needs to be addressed before a safe application of the method can be guaranteed is the verification of the maximum allowable stress that is exerted on HFMI-treated details concerning the stability of residual stresses generated by the method. Statistical analysis using the peak over threshold (POT) method together with more than one million measured lorries in Sweden and the Netherlands are used to calculate the maximum load effect from real traffic. The characteristic value of the maximum load is then compared to those obtained from the load model according to Eurocode for many beam bridges with different influence line shapes and lengths. The following conclusions have been made about the statistical analysis:

1. The use of the daily maxima as an object for extrapolation using the POT method is found to be justified for the studied traffic pools as most of the daily maxima belong to the absolute highest bending moment values.

2. The sensitivity of the selected threshold is found to be relatively low because the extreme value distribution is derived from the daily maxima which belong to the absolute maximum bending moment.

3. The Dutch traffic is found to be heavier than the Swedish one and produces a higher maximum bending moment because the former includes exceptional transport with heavy vehicles which requires special permits.

4. The curve fitting to the exponential distribution is found to be more accurate for the studied Swedish data pool because of the larger data pool size.

In addition, the following conclusion could be made about the maximum permissible stresses on HFMI-treated constructional details:

5. Considering the frequent combination, load model 1 is found to be suitable for representing Swedish traffic. Nonetheless, it underestimates Dutch traffic significantly.

6. The ULS combination overestimates the real traffic for both pools. Therefore, it is not appropriate for checking the maximum allowable stress.

7. The characteristic SLS combination is found to be best in representing real traffic but is still considered on the safe side in most cases.

8. Using this load combination, two case-study bridges were investigated where, in addition to traffic loads, permanent loads, thermal load, shrinkage effect, and wind load are considered. In none of these bridges did the maximum stress from the proposed load combination exceed the limit for tensile or compressive stresses assigned for HFMI-treated details.

9. The designer needs to take the maximum stress into account when HFMI treatment is used for fatigue strength enhancement. This can be made via the characteristic SLS combination of actions in the treated weldments positions.

10. More research is encouraged to provide similar verification formats for other welded structures that can be enhanced by HFMI treatment, such as railway and pedestrian bridges, cranes, or offshore structures.

Author Contributions: Conceptualization, H.A.-K. and M.A.-E.; methodology, H.A.-K. and J.L.; formal analysis, H.A.-K.; investigation, H.A.-K. and J.L.; resources, M.A.-E.; data curation, J.L.; writing—original draft preparation, H.A.-K.; writing—review and editing, J.L. and M.A.-E.; supervision, J.L. and M.A.-E.; project administration, M.A.-E. All authors have read and agreed to the published version of the manuscript.

Funding: This research was funded by Trafikverket and Vinnova. Besides, the article publication fees are provided by Brosamverkan.

Data Availability Statement: No data were created.

Acknowledgments: The authors are grateful for Trafikverket, Vinnova and Brosamverkan for their support.

Conflicts of Interest: The authors declare no conflict of interest.

Appendix A

The self-weight calculation is straightforward. Besides, Load model 1 consists of both concentrated and distributed loads. These loads should be placed to give the maximum action transversally and longitudinally. First, depending on the number of lanes, the loads are placed transversally so that the bending moment is maximized on one of the girders as shown in Figure A1. Then, the concentrated and distributed forces are calculated as given in the below equations. Next, the calculated forces are placed on the spans to generate the maximum action longitudinally.

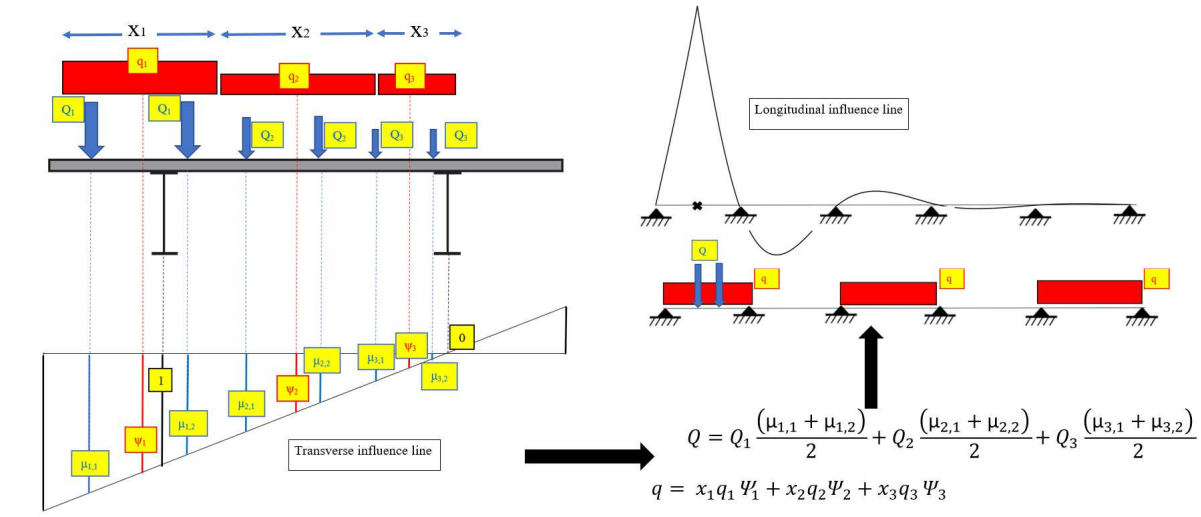

Figure A1. Consideration of traffic load model 1 transversally & longitudinally.

The wind force is applied on both the vehicle and the bridge girder. The average vehicle height is assumed to be 2 m. The direct effect of wind load is transverse bending which can be ignored owing to the relatively giant cross sections of the case study bridges. Moreover, the positioning of the wind loads relative to the shear center (assumed to be at the top girder) produces vertical moments which are combined with the other actions. The method of considering this moment is given in Figure A2.

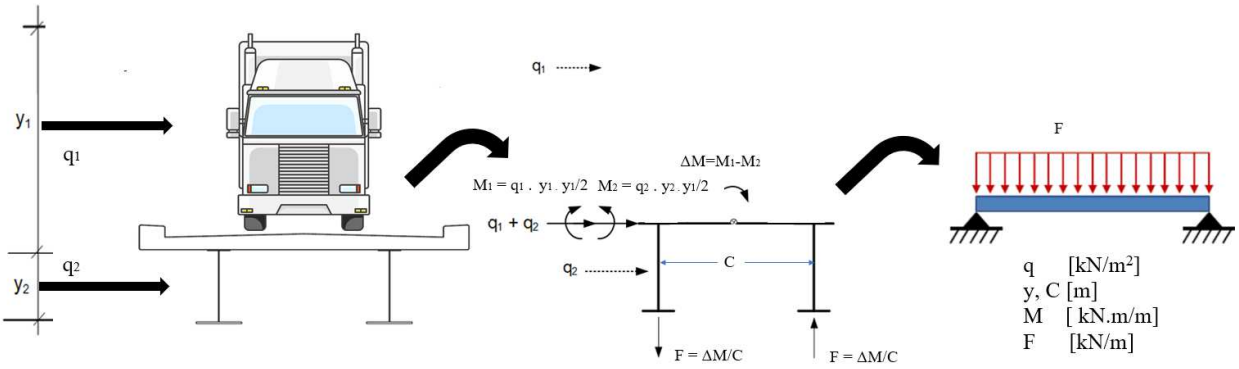

Figure A2. Load model to consider the bending moment generated by the wind load.

Drying and autogenous shrinkage strain are calculated to be 0.00246 in the ULS [25]. This generates tensile stresses in the concrete deck due to restrictions from movement. On the other hand, compressive stresses are generated in the girder. Besides, an additional bending moment is generated due to the misalignment of shrinkage force location to the center of the girder, see the Equation and the figure below. This applies to the simply supported bridge where the concrete deck is always under compression and considered to be uncracked. On the other hand, for continuous bridges, a design value of 25 MPa is applied for the compression stress in the lower flange in the cracked region (within 0.15 L from the internal support), and a corresponding value is estimated in the upper flange depending on the position on the neutral axis [25].

$$\varepsilon_{Shr} = 246.10^{-6}\ N_{Shr} = (Ec/n_{long}).A_c\ \varepsilon_{Shr}\ M_{Shr} = N_{Shr}\ (z\_conc\text{-}z\_comp)$$

$\varepsilon_{Shr} = 246.10^{-6}$ $N_{Shr} = (Ec/n_{long}).A_c\ \varepsilon_{Shr}$ $M_{Shr} = N_{Shr}\ (z\_conc\text{-}z\_comp)$

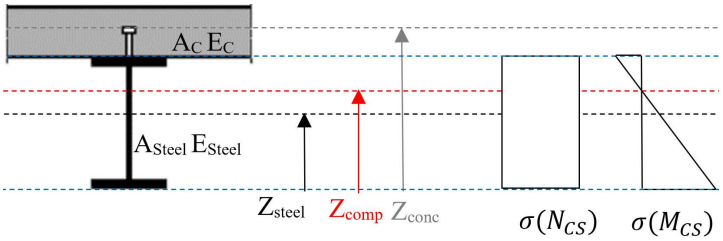

Figure A3. Shrinkage-induced stresses in the simply supported bridge (case study 1 in Figure 6).

Eurocode specifies a temperature difference of 10 °C acting at the center of the steel girder causing expansion or contraction [21]. This produces normal force and bending moment; see the below equations:

$\alpha = 10.10^{-6}$ $\Delta T = \pm 10$ °C F_Temp = $\varepsilon_{Temp} E_{Steel} A_{Steel}$ $M_{Temp} = F_{Temp}(Z\_Comp\text{-}Z\_Steel)$

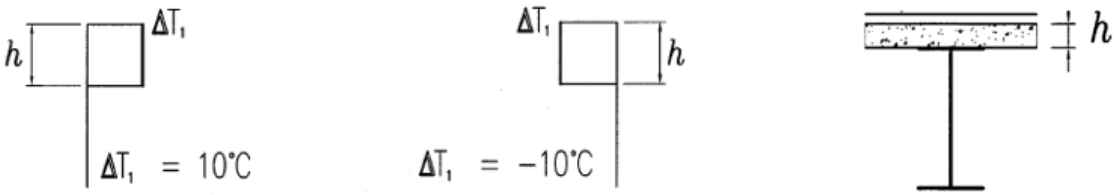

Figure A4. Considered thermal gradient of 10 °C [21].

References

1. Pedersen, M.M.; Mouritsen, O.Ø.; Hansen, M.R.; Andersen, J.G.; Wenderby, J. Comparison of post-weld treatment of high-strength steel welded joints in medium cycle fatigue. *Weld. World* **2010**, *54*, R208–R217. [CrossRef]
2. Yuan, K.L.; Sumi, Y. Modelling of ultrasonic impact treatment (UIT) of welded joints and its effect on fatigue strength. *Frat. Integrità Strutt.* **2015**, *34*, 476–486.
3. Al-Karawi, H.; Al-Emrani, M. Fatigue life extension of existing welded structures via high frequency mechanical impact (HFMI) treatment. *Eng. Struct.* **2021**, *239*, 112234. [CrossRef]
4. Al-Karawi, H.A. Fatigue life estimation of welded structures enhanced by combined thermo-mechanical treatment methods. *J. Constr. Steel Res.* **2021**, *187*, 106961. [CrossRef]
5. Al-Karawi, H.; Shams-Hakimi, P.; Al-Emrani, M. Mean Stress Effect in High-Frequency Mechanical Impact (HFMI)-Treated Steel Road Bridges. *Buildings* **2022**, *12*, 545. [CrossRef]
6. Maddox, S.J.; Doré, M.J.; Smith, S.D. A case study of the use of ultrasonic peening for upgrading a welded steel structure. *Weld. World* **2011**, *55*, 56–67. [CrossRef]
7. Leitner, M.; Stoschka, M. Effect of load stress ratio on nominal and effective notch fatigue strength assessment of HFMI-treated high-strength steel cover plates. *Int. J. Fatigue* **2020**, *139*, 105784. [CrossRef]
8. Leitner, M.; Khurshid, M.; Barsoum, Z. Stability of high frequency mechanical impact (HFMI) post-treatment induced residual stress states under cyclic loading of welded steel joints. *Eng. Struct.* **2017**, *143*, 589–602. [CrossRef]
9. Marquis, G.B.; Barsoum, Z. IIW Recommendations on high frequency mechanical impact (HFMI) treatment for improving the fatigue strength of welded joints. In *IIW Recommendations for the HFMI Treatment*; Springer: Singapore, 2016; pp. 1–34.
10. Gerster, P. Höherfrequente Hämmerverfahren–Vorstellung derneuen DASt-Richtlinie 026. 2019. Available online: https://docplayer.org/213556647-Hoeherfrequente-haemmerverfahren-vorstellung-der-neuen-dast-richtlinie-026.html (accessed on 10 January 2023).
11. Shams-Hakimi, P.; Al-Karawi, H.; Al-Emrani, M. High-cycle variable amplitude fatigue experiments and design framework for bridge welds with high-frequency mechanical impact treatment. *Steel Constr.* **2022**, *15*, 172–187. [CrossRef]
12. Kuhlmann, U.; Breunig, S.; Ummenhofer, T.; Weidner, P. Entwicklung einer DASt-Richtlinie für höherfrequente Hämmerverfahren: Zusammenfassung der durchgeführten Untersuchungen und Vorschlag eines DASt-Richtlinien-Entwurfs. *Stahlbau* **2018**, *87*, 967–983. [CrossRef]
13. Schubnell, J.; Carl, E.; Farajian, M.; Gkatzogiannis, S.; Knödel, P.; Ummenhofer, T.; Wimpory, R.; Eslami, H. Residual stress relaxation in HFMI-treated fillet welds after single overload peaks. *Weld. World* **2020**, *64*, 1107–1117. [CrossRef]
14. Ghahremani, K.; Walbridge, S.; Topper, T. High cycle fatigue behaviour of impact treated welds under variable amplitude loading conditions. *Int. J. Fatigue* **2015**, *81*, 128–142. [CrossRef]

15. Mikkola, E.; Remes, H.; Marquis, G. A finite element study on residual stress stability and fatigue damage in high-frequency mechanical impact (HFMI)-treated welded joint. *Int. J. Fatigue* **2017**, *94*, 16–29. [CrossRef]
16. Okawa, T.; Shimanuki, H.; Funatsu, Y.; Nose, T.; Sumi, Y. Effect of preload and stress ratio on fatigue strength of welded joints improved by ultrasonic impact treatment. *Weld. World* **2013**, *57*, 235–241. [CrossRef]
17. Pipiras, V. Pitfalls of data-driven peaks-over-threshold analysis: Perspectives from extreme ship motions. *Probab. Eng. Mech.* **2020**, *60*, 103053. [CrossRef]
18. Leander, J. Reliability evaluation of the Eurocode model for fatigue assessment of steel bridges. *J. Constr. Steel Res.* **2018**, *141*, 1–8. [CrossRef]
19. Maljaars, J. Evaluation of traffic load models for fatigue verification of European road bridges. *Eng. Struct.* **2020**, *225*, 111326. [CrossRef]
20. Carlsson, F. Modelling of Traffic Loads on Bridges Based on Measurements of Real Traffic Loads in Sweden. Ph.D. Thesis, Lund University, Lund, Switzerland, 2006.
21. *EN 1991-2*; Eurocode 1–Actions on Structures-Part 2: Traffic Loads on Bridges. European Committee for Standardization: Brussels, Belgium, 2003.
22. Mosiello, A.; Kostakakis, K. The Benefits of Post Weld Treatment for Cost Efficient and Sustainable Bridge Design. Master's Thesis, Chalmers University of Technology, Gothenburg, Sweden, 2013.
23. Shams-Hakimi, P. Fatigue Improvement of Steel Bridges with High-Frequency Mechanical Impact Treatment. Ph.D. Thesis, Chalmers Tekniska Hogskola, Gothenburg, Sweden, 2020.
24. Vrouwenvelder, T.; Holicky, M.; Markova, J. The JCSS probabilistic model code. *Struct. Saf.* **1997**, *19*, 245–251. [CrossRef]
25. Hirt, M.; Lebet, J.-P. *Steel Bridges: Conceptual and Structural Design of Steel and Steel-Concrete Composite Bridges*; CRC Press: Boca Raton, FL, USA, 2013.